# DEVELOPMENT OF LIGHT VEHICLE BRAKE PAD TEST RIG

**BY**

**YAMAN, Saraki Alhaji**
**(MEng/SEET/2016/6190)**

**DEPARTMENT OF MECHANICAL ENGINEERING**

**FEDERAL UNIVERSITY OF TECHNOLOGY**

**MINNA**

**JANUARY, 2020**

## ABSTRACT

This report presents the development of light vehicle brake pad test rig for testing and measuring the materials frictional characteristics such as brake pad wear rate, disc temperature, and average disc stopping time. Product validation and quality control is very necessary in the developmental process of any product. The brake pads were tested at various input variables such as speed and pressure to determine the effects of contact pressure on brake pad wear, and effects of speed on brake pad wear, disc temperature, and average stopping time. Two sets of brake pads designated as $pad_1$ (Semi Metallic pad) and $pad_2$ (Ceramic pad) were tested. At maximum disc speed (1400 rpm) and contact pressure (0.8 MPa), the wear rate of $pad_1$ is $4\times10^{-4}$ mm while $pad_2$ is $4.12\times10^{-4}$ mm both of which are lower than $5\times10^{-4}$ mm as reported by Blau, 2001. On varying the contact pressure, the wear rate of $pad_1$ and $pad_2$ at (0.8 MPa) are $3.9\times10^{-4}$ mm, $4.0\times10^{-4}$ mm respectively, and at (1.4 MPa) are $4.3\times10^{-4}$ mm and $4.4\times10^{-4}$ mm respectively. It was discovered that the wear rate increase as brake applied pressure increase. The $pad_2$ ceramic brake pad takes least time to stop on the average. On the average the disc temperature rise at any speed shows that $pad_1$ have high temperature rise in comparison with $pad_2$ which makes $pad_2$ a better brake pad.

## TABLE OF CONTENTS


| Title | Page |
|---|---|
| Title | ii |
| DECLARATION | Error! Bookmark not defined. |
| CERTIFICATION | Error! Bookmark not defined. |
| ACKNOWLEDGEMENTS | Error! Bookmark not defined. |
| ABSTRACT | ii |
| TABLE OF CONTENTS | iii |
| LIST OF TABLES | viii |
| LIST OF FIGURES | viii |
| ABBREVIATIONS, GLOSSARIES AND SYMBOLS | ix |
| **CHAPTERONE** | 1 |
| **1.0 INTRODUCTION** | 1 |
| 1.1 Background to the Study | 1 |
| 1.2 Statement of the research Problem | 2 |
| 1.3 Justification of the Study | 2 |
| 1.4 Aim and Objectives of the Study | 3 |
| 1.5 Significance of the Research | 3 |
| 1.6 Scope of the Study | 4 |

1.7 Limitations of the Research 4

**CHAPTER TWO** 5

**2.0 LITERATURE REVIEW** 5

2.1 Braking System 5

2.1.1 Major components in the braking system 6

2.1.1.1 Disc brake assembly 6

2.1.1.2 Drum brakes assembly 6

2.1.1.3 Brake fluid 7

2.1.1.4 Direct servo system. 7

2.2 Braking Fundamentals 8

2.2.1 Energy of motion 8

2.2.2 Coefficient of friction 8

2.2.3 Stopping distance 9

2.2.4 Brake torque. 9

2.2.5 Braking efficiency 9

2.3 Brake Pads 10

2.3.1 Types of brake pads 10

2.3.1.1 Organic brake pads 11

2.3.1.2 Ceramic brake pads 11

2.3.1.3 Metallic brake pads 11

2.4 Traditional Brake Testing 11

2.5 Brake Material Testing Facilities 12

2.6 Operating Condition 14

2.6.1 Measuring the brake temperature 14

**CHAPTER THREE** 16

**3.0 MATERIALS AND METHODS** 16

3.1 Materials 16

3.1.1 Equipment 16

3.3 Design Description 17

3.4 Operating Principle of the Brake Pad Test Rig 18

3.5 Determination of Power Required 19

3.5.1 Power transmitted by the shaft 21

3.6 Determination of Shaft Diameter 23

3.6.1 Determination of shaft diameter due to only twisting moment 23

3.6.2 Shaft diameter due to bending and twisting moment 24

3.6.3 Shaft diameter according to standard practice 26

3.7 Design of Shaft Coupling 30

3.7.1 Determination of hub diameter 30

3.7.2 Determination of hub length 31

3.7.3 Determination of hub thickness 31

3.7.4 Determination of hub key length 31

3.7.5 Determination of hub key width 32

3.8 Bearing Selection 32

3.9 Frame Design 37

3.9.1 Critical buckling load 37

3.10 Material Selection 40

3.11 Fabrication Details 42

3.11.1 Cutting and shaping 42

3.11.2 Assembling 42

3.12 Machine Parts Description 43

3.12.1 Shaft 43

3.12.2 Flywheel 43

3.12.3 Coupling 43

3.12.4 Servo 43

3.12.5 Frame 43

3.13 Testing Procedure 44

3.14 Methods of Measuring Wear 45

3.15 Cost Analysis 45

3.15.1 Material cost 45

3.15.2 Total cost of construction 47

**CHAPTER FOUR** 48

**4.0 RESULTS AND DISCUSSION** 48

4.1 Results 48

4.1.1 Design results 48

4.1.2 Wear test results 48

4.1.3 Disc stopping time results 49

**CHAPTER FIVE** 54

**5.0 CONCLUSION AND RECOMMENDATION** 54

5.1 Conclusion 54

5.2 Recommendations 55

REFERENCE 56

APPENDICES 59

## LIST OF TABLES


| Table | | Page |
|---|---|---|
| 3. 1 | Materials used for the development and testing of the test rig | 16 |
| 3. 2 | Equipment used for this testing Apparatus | 17 |
| 3. 3 | Electric Motor Efficiency | 18 |
| 3. 4 | Principal dimensions for radial ball bearings | 24 |
| 3.5 | Values of $f_c$ for different types of bearings | 27 |
| 3. 6 | Recommended Life Value of Bearings. | 36 |
| 3. 7 | List of materials used with price. | 46 |
| 4. 1 | Effect of Speed on Brake Pad Wears at Constant Brake Pressure (0.80Mpa) After Ten of Brake Operation | 48 |
| 4. 2 | Effect of Brake Contact Pressure on Brake Pad Wears at Constant Speed (1400rpm) After Ten Sequence of Brake Applicattions | 49 |
| 4. 3 | Effect of Speed on Average Stopping Time of The Disc at Constant Contact Brake Pressure (0.80MPa) After Ten Sequence of Brake Applications | 49 |
| 4. 4 | Effects of Speed on Temperature of the Disc at Constant Contact Pressure (1.60MPa) After Ten Sequence of Brake Applicationss | 50 |

## LIST OF FIGURES

**Figures** **Pages**


2.1: A typical braking system 5

2. 2 Direct-acting servo. A. Brake being applied or fully applied. B. Brake held on. 7

3. 1 Schematic diagram of experimental brake pad test rig 18

3. 2 Free Body Diagram of the Rotating Shaft 24

3. 3 Shear forces and bending moment diagram 27

4. 1 Effect of Disc Rotational Speed on Brake Pad Wears at Invariable Pressure (0.80MPa) After Ten Sequence of Brake operations 51

4. 2 Effect of Brake Pressure on Pads Vertical Height Reduction at Constant Speed (1400rpm) After Ten Sequence of Brake operations. 51

4. 3 Effect of Disc Speed on Average Stopping Time taken at Constant Contact Brake Pressure (0.80MPa) After Ten Sequence of Brake operations 52

4. 4 Effects of Speed on Temperature of the Disc at Constant Contact Pressure (1.60 MPa) After Ten Sequence of Brake operations 53

## ABBREVIATIONS, GLOSSARIES AND SYMBOLS

| NOTATIONS | SYMBOLS | UNITS |
|---|---|---|
| Acceleration | A | $m/s^2$ |
| Acceleration due to gravity | G | $m/s^2$ |
| Angular speed | W | rev/s |
| Average radius of brake pad | | m |
| Bearing axial or thrust load | Y | - |
| Bearing basic dynamic radial | C | N |
| Bearing basic static radial load | $C_0$ | N |
| Bearing bore diameter | B | mm |
| Bearing constant axial or thrust | $W_A$ | N |
| Bearing constant radial load | $W_R$ | N |
| Bearing diameter average | $d_m$ | mm |
| Bearing dynamic equivalent | | - |
| Bearing geometrical factor | $f_c$ | - |
| Bearing life in working hours | $L_H$ | Hours |
| Bearing nominal angle of | A | degree ($^o$) |
| Bearing number of ball per row | Z | - |
| Bearing outside diameter | A | mm |
| Bearing radial load factor | X | - |
| Bearing rating life | L | rev |
| Bearing rotation factor | V | - |

| | | |
|---|---|---|
| Bearing type factor | $f_0$ | - |
| Bending moment | M | Nm |
| Bending stress | $\boldsymbol{\sigma}$ | $N/m^2$ |
| Bending stress | $\boldsymbol{\sigma}_b$ | $N/m^2$ |
| Brake pad contact surface area | | $m^2$ |
| Brake pressure | P | MPa |
| Braking moment | M | Nm |
| Ceramic Pad | $Pad_2$ | - |
| Coefficient of friction | μ | - |
| Combined shock and fatigue | $K_b$ | - |
| Combined shock and fatigue | $K_t$ | - |
| Constant | K | - |
| Critical frequency of transverse | $f_n$ | Hz |
| Critical load | $\omega_{critical}$ | N |
| Deflection | $\delta$ | mm |
| Disc force | $F_{disc}$ | N |
| Disc radius | $r_{disc}$ | mm |
| Distance | S | M |
| Eccentricity | E | mm |
| Elastic modulus for iron | $\mathbf{E_i}$ | Gpa |
| Equivalent twisting moment | Te | Nm |
| Factor of safety | N | - |

| | | |
|---|---|---|
| Final velocity | V | m/s |
| Flywheel radius | $R_{f;luwheel}$ | m |
| Force | F | N |
| Force of disc | $F_{disc}$ | N |
| Force of flywheel | $F_{flywheel}$ | N |
| Frictional force | $F_{friction}$ | N |
| Hub diameter | $d_1$ | mm |
| Hub key length | $L_K$ | mm |
| Hub key width | $W_K$ | mm |
| Hub length | $L_H$ | Mm |
| Hub thickness | $t_1$ | Mm |
| Initial velocity | U | m/s |
| Kinetic energy | $k_E$ | J |
| Kinetic Energy | $K_E$ | J |
| Length of the column | $L_C$ | Mm |
| Lower moment of inertia for the | $\mathbf{I_R}$ | $\mathbf{m^4}$ |
| Mass | M | Kg |
| Mass | M | Kg |
| Mass of disc | $M_{disc}$ | Kg |
| Mass of flywheel | $M_{flywheek}$ | Kg |
| Moment of inertia of rotor | I | $m^4$ |
| Motor efficiency | $\eta_m$ | - |

| | | |
|---|---|---|
| Natural frequency | $\omega_n$ | rev/s |
| Normal force | $F_{normal}$ | N |
| Number of ball per row | Z | - |
| Number of row | I | - |
| Polar moment of inertia | J | Nm |
| Power in to the motor | P | Watts |
| Power transmitted by the shaft | P | Watts |
| Radius | R | m |
| Semi Metallic pad | $Pad_1$ | - |
| Shaft diameter | D | M |
| Shaft length | L | m |
| Shaft power out | $P_{out}$ | Watt, W |
| Shaft speed | N | Rpm |
| Shaft torque | $T_s$ | Nm |
| Shear force | V | N |
| Shear stress | $S_s$ | $N/m^2$ |
| Shear stress | $V_a$ $V_b$ Vd | $N/m^2$ |
| Shear stress | | MPa |
| Static deflection | Y | mm |
| Time | T | s |
| Time | T | S |
| Torque of disc | | Nm |

| | | |
|---|---|---|
| Torque of flywheel | | Nm |
| Total torque of system | T | Nm |
| Vertical reaction force | $R_{BV}$ , $R_{FV}$ | N |

# CHAPTER ONE

## 1.0 INTRODUCTION

### 1.1 Background to the Study

The utilization of motor vehicles as among other means of shipping on roads and other compliant surfaces cannot be over stressed and has been an essential component of daily performances. An important reflection for secure, successful function and restraint of these motor vehicles is the braking mechanism which must be capable of slowing down the vehicle at a quicker rate than the engine can speed it up (Aderibigbe *et al*., 2016). The two varieties of braking mechanism are: the drum brakes and the disc brakes. Motor vehicle utilised either of the two braking system or both the drum brakes and disc brakes, the main parts of a disc brake are among other frictional brake pads, rotor, and calliper. The critical component of any braking mechanisms is frictional brake fabric. It is as a result critical to prove the activities of the frictional associate in laboratory tests and working trial

( Systemtechnik, 2017).

The activities of the frictional brake fabric must meet least desires for wear, sound and toughness (Deepika *et al*., 2013). Disc braking mechanism consist of brake pad frictional fabric that must be changed time to time after wearing (Deepika *et al*., 2013). The performance of braking mechanism is limited by factors such as driver attitude, vehicular utilization, brake pad fabrics, the terrain where the vehicle is being used, vehicle gross weight, and also among others the mal adjustment of brake calliper (Nwufo *et al*., 2013).

Vehicular kinetic energy is transformed to heat energy generated in brake mechanism within 5 – 15 s, which is the typical time taking when applying brake from a reasonable small speed to the full stoppage. Heat energy released between the surfaces in contact affect the brake performance (Hwang *et al*., 2008). Defects on the surface, which may be due to profile errors and geometric formation, may be the reason for uneven temperature distribution.

### 1.2 Statement of the Research Problem

The experimental brake pad test rig apparatus are scarce and expensive in nation like Nigeria. Therefore, development of inexpensive test apparatus using local material comes up. A lot of frictional engineering materials (specifically brake pads) are being developed in institutions of higher learning and needed to be tested for validation. This study centres on the developing brake pad test apparatus to cater for this demand and serve as sources of validating performance and durability of motor vehicle frictional brake pad by replicate the braking mechanism on which the pads are to be used.

### 1.3 Justification of the Study

Testing of engineering materials is a paramount step in any developmental process of products or experimental research in general. Developing countries like Nigeria are far behind in terms of product development making it difficult for researchers when verifying validity of the research carried out or testing the various properties of materials produced from various researches. This machine will serve as a means to fill this gap. Millions of dollars are being spent on buying of testing equipment and even test being sent to foreign countries by various researchers in institutions of higher learning across the country, the

test rig being developed will be a source of furthering our own local content, improving home production industries thereby relieving difficulties faced by researchers.

### 1.4 Aim and Objectives of the Research

The aim of this research work is to develop and carry out performance evaluation of light vehicle brake pad test apparatus.

The objectives are:

1. To design a brake pad test rig
2. To fabricate a brake pad test rig.
3. To carry out performance assessment of the brake pad test rig.

### 1.5 Significance of the Research

Local manufacturing is the key to the industrial revolution needed in Nigeria. Validation and property control of any product is very vital in process of the product development. The product could be a machine or an engineering material. Today in our Nation research institutes, researchers have been working on frictional materials with a view to find a more reliable and competitive frictional materials with good frictional properties that could possibly replace the existing original equipment manufacturers (OEM) brake pad materials using local materials which needs testing. The method use for evaluation of these brake lining is through full vehicle test which is expensive, since this brake pad full vehicle test is expensive, it has become necessary to develop a laboratory method for quick, low cost and effective evaluation of brake linings for validation.

## 1.6 Scope of the Research

This work deals with the development of a brake pad testing apparatus to discover the effect of surface contact pressure on brake pad wear, effect of speed on brake pad wear, effect of speed on average stopping time of the disc and on disc temperature.

## 1.7 Limitations of the Research

Estimating some frictional properties of brake pad requires versatile apparatus such as vastly susceptible revolution measuring instrument, temperature measuring instrument, and brake applied pressure gauge which are rare and costly, some accessible apparatus for estimating brake pad frictional properties were utilized to accomplish the research objectives.

# CHAPTER TWO

## 2.0 LITERATURE REVIEW

### 2.1 Braking System

Motor vehicle braking mechanism is an assembly of majorly electronic, hydraulic and mechanical stimulated parts. It utilizes friction between the pads and brake disc to bring vehicle in motion to a standstill (Bhandari, 2010). As the brake pedal is depressed, master cylinder piston travel to the other end to force the fluid contain in the master cylinder through brake fluid hose which activate the callipers and wheel cylinders (http://motorist.org/articles/auto-braking-systems). The applied brake force on the brake pedal creates a relative force on each of the pistons. A figure of the braking system is shown in Figure 2.1 highlighting the major components.

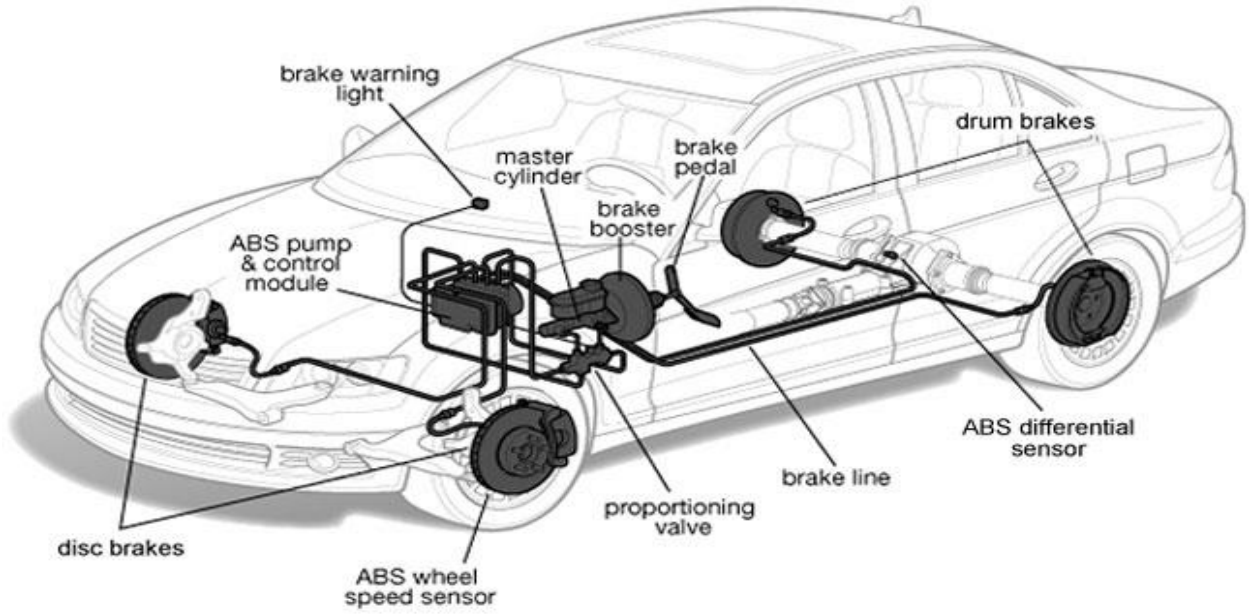


Figure 2.1: A typical braking system (Source: http://www.levintirecenter.com/car-brake-system.html)

The brake mechanism of automobile vehicle consists of piston which is attached to either brake shoe or brake pad. The piston travel to the other end thereby moving fixed brake pad frictional material against rotating surface of the disc or drum to reduce wheel rotation (Kost, 2014). As brake pedal depressed is released, the pads or shoe of the brake go back to their free position and the brake fluid also return back to master cylinder through the fluid hose (Jamie, 2008).

### 2.1.1 Major components in the braking system

According to Idris *et al.* (2015) the major components of a braking system are the disc brake assembly, drum brake assembly, brake fluid and Servo System.

#### 2.1.1.1 Disc brake assembly

The disc brake assembly is consisting of brake components like rotor, bearing, frictional brake pads, calliper mechanism and fasteners needed to climb the component parts on the vehicle. The brake fluid line attached to the calliper and to the master cylinder carries the brake fluid through the brake mechanism (Idris *et al.,* 2015).

#### 2.1.1.2 Drum brakes assembly

According to the Universal Swillington tyres and auto centre website, the drum brake assembly is also consisting drum, shoes, bearings, wheel cylinder, backing plate and hub sub assembly and fasteners needed to climb the component parts on the vehicle. The brake fluid line and valves attached to the master cylinder carries the brake fluid through the braking mechanism (Idris *et al.,* 2015).

### 2.1.1.3 Brake fluid

The brake fluid is a kind of hydraulic oil makes use of in motor vehicles and also semi heavy duty trucks. This fluid conveys applied pressure to the braking system closer to the wheels through brake fluid line (CDX Automotive, 2012). For successful and efficient braking, the brake fluid must not lack high boiling point because braking operation generate a lot of heat energy (CDX Automotive, 2012).

### 2.1.1.4 Direct servo system.

The direct servo system used either single or cycle master cylinders (Systemtechnik, 2017). The servo is fixed to the linkage of the brake pedal. The unit, shown in Figure 2.2, shows the condition where the mechanism is operating, while the brakes are not operating and servo piston is hanged in the vacuum. The air in the air compartment is delivered to the engine manifold with the help of the pipe and the valve fit next to the vacuum cavity. The piston is closed by the control valve which is linked to brake applied pedal (Xiao *et al.*, 2016).

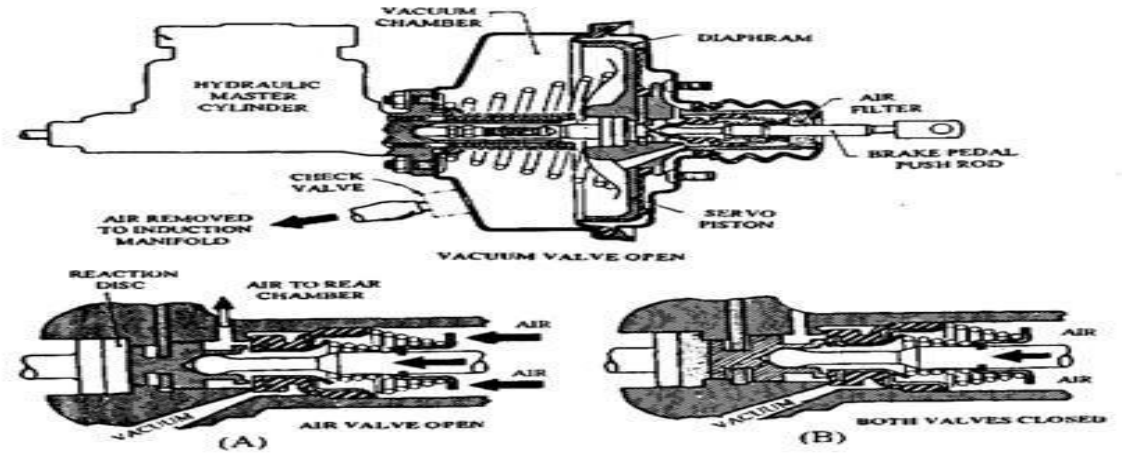


s

Figure **2. 2** Direct-acting servo. A. Brake being applied or fully applied. B. Brake held on. (Source: http://motorist.org/articles/auto-braking-systems).

## 2.2 Braking Fundamentals

### 2.2.1 Energy of motion

The energy of motion of a vehicle is the power that maintains the moving vehicle. The vehicle engine provides this kinetic energy so as to speed the vehicle from an idle to required speed. This energy is dissolved as heat by the brakes during brake application. The kinetic energy K of a vehicle for the period of braking is given by Equation 2.1(Chatterton *et al.*, 2016).

$$K_E = \left(\frac{1}{2}\right) M(V^2 - U^2) \quad (2.1)$$

### 2.2.2 Coefficient of friction

Friction resists the movement of motor vehicle, since this expend energy, heat is produced (Gupta, 2014). Road wheel rotation is resisted by brake application and friction takes place amid complaint surface and wheel tyre. Commuter car brakes have 0.3 to 0.5 as the friction coefficient between the tyre and plane surface (Gupta, 2014). Coefficient of friction and other factors such as brake pad surface area, shoe geometry and brake depressed pressure is critical in the absorption of heat energy. Abrupt or unexpected brake application cause high heat energy generated. Van-Iersel (2006) employed a coefficient of friction of 0.5 to measure the frictional behaviour of different materials using the TR3 test bench test rig. Coefficient of friction can be determined from Equation 2.2 (Hoodbhoy, 2014).

$$\mu = \frac{F_{friction}}{F_{normal}} \quad (2.2)$$

Van-Iersel (2006) modified Equation 2.2 to Equation 2.3 for use in the TR3 test rig.

$$\mu = \frac{M_{brake}}{R_{av}\, pA_{pad}} \quad (2.3)$$

### 2.2.3 Stopping distance

Stopping distance also known as braking distance is the distance a vehicle will travel from the point when the brakes are entirely applied to when it comes to complete stoppage. It is vital for urgent brake application. Braking distance is influenced by braking effort applied by the driver and tyre deflection. Equation 2.4 is used to determine braking distance at 100% brake efficiency

$$S = ut + \frac{1}{2}\, at^2 \quad (2.4)$$

Koop (2012) explained that there are two basic ways to measure stopping distances: physically measure the distance it takes the vehicle to stop at a specific speed or use an instrument that tells you the stopping distance as a digital readout, calculated by converting deceleration forces more commonly known as "G" forces into a stopping distance. With similar road wheel tyre and plane surface condition, the braking space stays equal when the brake pedal is depressed while the wheels are locked and skid irrespective of vehicle hardware or its total weight. Braking force is utmost prior to the brake locking that is the point when skidding is about to occur. Anti-lock brake system activate just before this point.

### 2.2.4 Brake torque.

The force applied at the braking system to resist the motion of rotating system or apparatus is known as braking torque. The needed torque is established by effective axle height and

stopping force amid the road plane surface and the road wheels. (Hoodbhoy, 2014). Knuckle and suspension control arm absorbed front brake torque while axle housing and leaf spring absorbed the back braking torque. Braking force for urgency is higher than throttle accelerating torque (Koop, 2012). Brake hardware must possess good mechanical properties like toughness and strength to resist braking load.

### 2.2.5 Braking efficiency

The rotation of the vehicle wheel is resisted when the brake pedal of the vehicle is depressed, it therefore, lower its acceleration to return it to rest. This mean that the braking power is the power employed to diminish motor vehicle speed. Brake efficiency is the braking power generate as fraction of entire motor vehicle mass as given in Equation 2.5.

(Gudmand *et al.,* 1999).

$$\text{Braking efficiency}, \eta = \frac{\text{braking force}}{\text{weight of vehicle}} \times 100 \qquad (2.5)$$

Normally, brake power efficiency is less than 100% due to inadequate road adhesion, non-effective brake mechanism. Friction coefficient is comparable with brake efficiency which is the ratio of the frictional force to the normal weight between the contacting surfaces.

## 2.3 Brake Pads

There are different types of brake pad products from metallic brake pads, ceramic brake pads to organic brake pads accessible in the market. Brake pads are component part of any disc brake system use to create a friction between contacting surfaces which reduce or bring to a halt the rotation (Jamie, 2008).

### 2.3.1 Types of brake pads

There are three major types of brake pads, categorized by the materials used to make them.

#### 2.3.1.1 Organic brake pads

The materials of organic brake pads are glass, rubber and resin which has a property to resist utmost heat. Non asbestos as it is sometime called resist the high heat in binding its fibre simultaneously (Amaren, 2013). According to Jamie (2008) non asbestos brake pads are non-hazardous, quieter among other good qualities of these organic brake pad materials however, they wear much faster, produce powder dust.

#### 2.3.1.2 Ceramic brake pads

The materials that are used to prepare ceramic brake pads are ceramic fibre as matrix material, filler material and binding agents with little percentage of copper fibre (Jamie, 2008). The benefits of ceramic brake pads material over other brake pads materials include lightweight, utmost accomplishment while braking and it also disperses heat properly resulting to high braking performance after so many cycle of brake application

#### 2.3.1.3 Metallic brake pads

Metallic brake pad product is composite with iron as its matrix material and some percentage of steel, copper and graphite. Metallic brake pad products are not too expensive as compare with ceramic brake pads which makes it a popular choice amongst car users (Jamie, 2008). The downside of metallic brake pads is that they are heavy, and this leads to a negative impact on the cars fuel economy, high-performance driving and result in more wear on the brake rotors than other types of brake pads.

### 2.4 Traditional Brake Testing

Van-Iersel (2006) asserted that the traditional way of testing disc brakes by various researchers is to use an electromotor to speed the disc up to a desired amount of revolutions

per minute, while the disk is on the same axle with a number of flywheels. These flywheels should have the same moment of inertia as the vehicle that would normally carry the tested brake disks. After speeding up the disc the electromotor would be shut off and the brake would be applied. At this point the torque on the axle is measured by a sensor. From this measured braking torque, together with the braking pressure applied to the hydraulic fluid line and the dimensions of the brake disc and pads, the friction coefficient between the disc and the pads can be calculated.

### 2.5 Brake Material Testing Facilities

Many challenges are involved in the development of new generation materials to be used for automotive brake applications, including formulation of materials that address cost reduction; expected (usually more demanding) performance; and compliance with new safety and environmental regulations (Fecher*et al*., 2014). Brake materials are tested on brake test rigs that simulate a real vehicle stopping condition and complete characterization of frictional materials.

Testing of friction materials for brake applications is a cost- and time-intensive, it requires the rotor and brake pads to be in their final stage to properly simulate the brake system. To reduce some of the cost and difficulty, scaling down a test rig to simulate a brake system is sometimes necessary. The major critical physical parameters to be monitored for the tests according to Fecher *et al*. (2014) are sliding speed, friction, wear, vibration and temperature. The tribological performance of small, friction material samples can be characterized in a precise and timely manner.

Triches *et al*. (2004) used a brake inertia dynamometer to test the squeal noise from disc brake systems using constrained layer damping. The test rig consisted of a system of flywheels mounted onto a common central shaft to simulate the mass of the test vehicle. The minimum inertia is the inertia of the shafts, couplings, and disc brake, and the variable inertia is obtained by engaging the appropriate flywheels (Triches *et al*., 2004). The test rig flywheels were engaged manually with a support and transfer system using electromagnetic clutches. The dynamometer tests conducted by Triches *et al*. (2004) allowed for the controlling of parameters such as rotation, braking pressure and temperature (simulating real behaviour of a brake system in practice) while recording the sound pressure level and frequency of noise occurrences. Another test rig was developed by Nwufo *et al*. (2013) to determine the wear rate of a brake pad. It consists of a brake disc and calliper assembly, brake booster and master cylinder unit. The prime mover used was an electric motor, which drove a main driveshaft incorporating a flywheel weight and a mechanical actuator. The brake disc was mounted on the main shaft driven by the prime mover, while the calliper, the mechanical actuator and some other components were bolted to the frame of the rig. The flywheel enabled the inertia of a vehicle to be simulated and thus boosted the shaft's inertia when it is driven by the motor. The rig also incorporated a hydraulic circuit fitted with a pressure gauge to measure the pressure in the fluid line from which the force with which the brake pads push against the disc can be estimated. A boosting device (servo unit) was added to the hydraulic line. Two sets of brake pads from different manufacturers were tested on test rig by Nwufo *et al*. (2013). The test was carried out in two phases ,first by keeping contact pressure constant and varying rotating speed of the brake disc (ranging from 695 to 1248 rpm), and secondly by keeping speed of rotation constant and varying contact pressure (ranging from 0.8 to 1.4 MPa).

The average wear rate of the pads at a constant pressure of 1 MPa as obtained by Nwufo *et al*. (2013) was $6.115\times10^{-3}$ mm per brake application and $7.205\times10^{-3}$mm per brake application. These values are slightly higher than the average wear rate of a typical automotive brake pad material, that is, $5\times10^{-4}$ mm per brake application as reported by Blau (2001). At constant speed, the wear rates were $6.9\times10^{-3}$ mm per brake application for pad A while that of pad B is $8.05\times10^{-3}$ mm per brake application. The test rig used to test the new frictional material developed from palm kernel shells by Ibhadode and Dagwa (2008) was designed and developed by Dagwa, (2005). It had a 2.2 kW motor with a provision for speed variation by using a stepped pulley. The speed and brake line pressure ranges were: 6.66 m/s to 13.82 m/s and 0.2 – 0.6 MPa respectively for the test conditions. The comparisons for disc temperature rise and stopping time shows that the palm kernel brake pad developed by Ibhadode and Dagwa (2008) has the same performance as the commercial pad which include organic, ceramic and metallic brake pads. The average disc temperature rise and average stopping time for the palm kernel pad are 11.6ºC and 4.1s respectively, while the corresponding values are 13.1ºC and 4.2 s for the commercial pad.

### 2.6 Operating Conditions

To compare brake pads of different materials under various circumstances, Van-Iersel (2006) selected the specific operating conditions for load (Brake pressure from 1 to 4 MPa), speed (rotational speed of the disk, directly related to the car speed, 60 and 120 km/h.

#### 2.6.1 Measuring the brake temperature

Temperature is one of the most important parameters influencing the behaviour of the brake. The brake disc is heated by operating the brake, since friction generates heat. Van-Iersel (2006) in its experiment identified that the temperature at the brake surface depend

upon the brake torque. To obtain a more accurate result, Ivens (2007) suggested that the temperature should be measured closer to the brake pads. In real-life conditions, the brakes are cooled by natural convection which is influenced by driving speed. In the setup by Ivens (2007), this is simulated by blowing pressurized air along the brake. To make this effect more realistic as well, it should be dependent on the car's velocity.

In conclusion, this design has a similar feature to that design by Nwufo *et al*. (2013) with the exception of a protective transparent casing which is introduced to cover the rotating parts such as shaft, flywheel and brake assemble to avoid or prevent chips from flying. Heat is generated as the brake is applied and the temperature is one of the most important consideration which influences the behaviour of the brake. To measure the exact temperature rise of the disc after certain brake applications infrared (Noncontact) tachometer is introduced in this design for accurate temperature measurement So, to compare performance of different commercially available and newly researched brake pad materials, brake pads are subjected to the same operating conditions of brake pressure (load) ranges from 0.6 to 1.4 MPa.

# CHAPTER THREE

## 3.0 MATERIALS AND METHODS

### 3.1 Materials

The materials used for development of the brake pad apparatus are presented in Table 3.1

**Table 3. 1 Materials used for the development and testing of the test rig**

| S/N | Items | Materials | Specifications (mm) |
|---|---|---|---|
| 1 | Angle bar | Mild Steel | 50×50×4 |
| 2 | Shaft | Mild Steel | 360×25 |
| 3 | Couplings | Mild Steel | 4 |
| 4 | Cables | Copper | 12801 |

#### 3.1.1 Equipment

The equipment used for this testing apparatus are presented in Table 3.2

**Table 3. 2 Equipment used for this testing Apparatus**

| S/N | Items | Models | Descriptions |
|---|---|---|---|
| 1 | Electric Welding Machine | Maxm,Chtg/Nma<br>400,400,380 Volts | |
| 2 | Lathe | | |
| 3 | Hand Grinding Machine | | 125 mm Grinding Disc Diameter |
| 4 | Pressure Gauge | | 0 MPa - 1.6 MPa |
| 5 | Tachometer | | LCD Display Tachometer |
| 6 | Thermometer | | LCD Display Thermometer |
| 7 | Vanier Calliper | | Digital Vanier Calliper |
| 8 | Stopwatch | | Android Stopwatch |

### 3.2 Design Requirements

It is required that this design demonstrate the required performance of experimental brake pad test rig using different types of brake pad materials such as semi metallic brake pad material, ceramic brake pad material, low metallic brake pad material and any new developed brake pad materials. Manufacturing technologies connected with this product design is Peugeot 406 brake assembly and flywheel used to simulate the vehicle inertia.

### 3.3 Design Description

The setup drawing of the apparatus is as illustrated in the Figure 3.1. The rig major parts are: electric motor, couplings, flywheel, shaft, bearings, caliper assembly, and brake servo. The frame made of angular iron was used to house all the test rig parts. The shaft was fixed

axially with the shaft of electric motor to transmit the rotary motion of the electric motor via couplings, while the flywheel was situated centrally between the two bearings. The flywheel was used to simulate the vehicle inertia. The caliper assembly comprises of the disc, caliper, brake pads, pressure gauge, fluid (hydraulic) line, and fluid reservoir directly connected to the pressure gauge for brake applied pressure measurement. The brake servo is incorporated to boost the brake applied pressure.

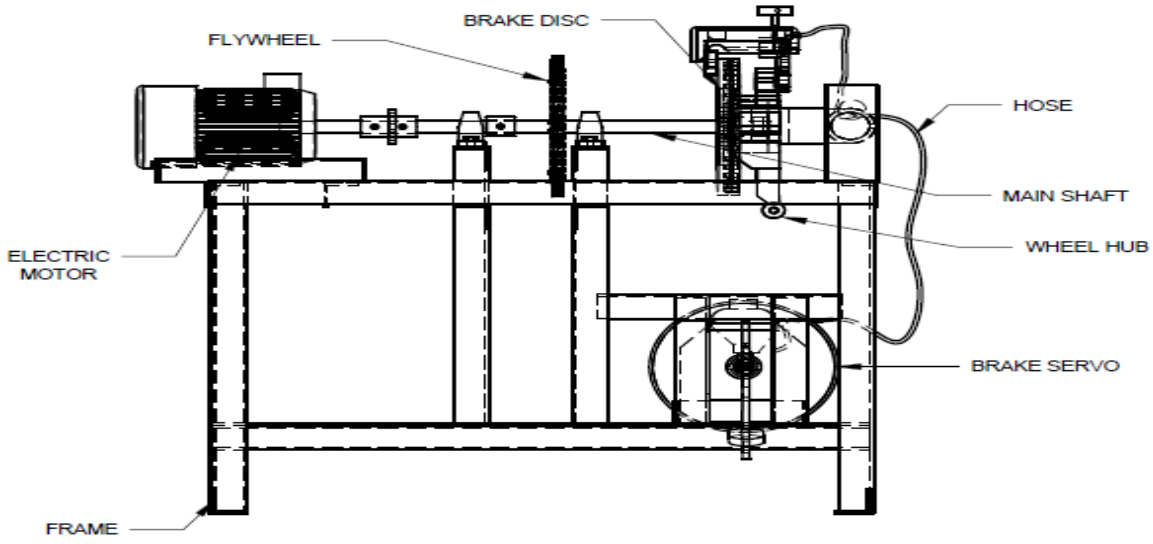


Figure 3. 1 Schematic diagram of experimental brake pad test rig

(Source: Working drawing)

### 3.4 Operating Principle of the Brake Pad Test Rig

First a set of brake pads to be tested will be coupled into the calliper of the brake assembly. The shaft will then be set in motion by the electric motor. The disc and flywheel both will rotate until a stable speed of motor is achieved. When the speed stabilizes at 1400 rpm, the switch will then be turned off while the motor, flywheel, disc and the shaft rotates by virtue of their inertia then the brake will be applied mechanically by depressing the brake pedal

with the foot until it is brought to rest via the action of the pads against the disc. As this is done, the time taken for the shaft to come to rest will be measured and recorded. After the test, the brake pads will be brought out for visual inspection and measurements for wear in terms of reduction in thickness. The test will be carried out at different speeds and different brake pressure such as 1400, 1200, 1000, 800 and 600 rpm and 0.6, 0.8, 1.0, 1.2, and 1.4 MPa respectively with the help of brake pressure gauge and tachometer. The speed and brake pressure variations are to help find the effects of speed and pressure on brake pad wear rate.

### 3.5 Determination of Power Required

The power required to propel the system can be obtained using Equation 3.1, and the torque is given by Equation 3.2 (Khurmi and Gupta, 2005).

$$\text{Power} = \frac{2\pi NT}{60} \tag{3.1}$$

$$\text{Torque} = F \times r \tag{3.2}$$

Two masses are used in the setup, mass of disc and mass of fly wheel. The flywheel is incorporated to simulate the vehicle inertia. Radius of disc used is 140 mm and the mass of brake disc used is 8.4 kg, therefore, the Normal force on the shaft due to weight of the brake disc from Equation 3.3 was calculated as 82.4 N

$$F_{disc} = m_{disc} \times g \tag{3.3}$$

$$F_{disc} 8.4 \times 9.81$$

$$F_{disc} = 82.4 \text{ N}$$

$$T_1 = F_1 \times r_1 \quad (3.4)$$

$$T_1 = 82.4 \times 0.14$$

$$T_1 = 11.5 \text{ Nm}$$

The radius of flywheel used is 145 mm and the mass of flywheel used is 8 kg, therefore, the Normal force on the shaft due to weight of the flywheel from Equation 3.5 was calculated as 78.5 N

$$F_{flywheel} = m_{flywheel} \times g \quad (3.5)$$

$$F_{flywheel} = 8 \times 9.81$$

$$F_{flywheel} = 78.5 \text{ N}$$

$$T_2 = F_2 \times r_2 \quad (3.6)$$

$$T_2 = 78.5 \times 0.145 = 11.4 \text{ Nm}$$

$$T = T_1 + T_2 \quad (3.7)$$

$$T = 11.5 + 11.4 \quad T = 22.9 \text{ Nm}$$

The total torque of the system is the sum of both torques obtained.

T = 22.9 Nm

Speed adopted for the design calculations is 1400 rpm as this is the maximum speed of the electric motor which will give this design considerable accelerated brake pad wear for analysis (Nwufo *et al.*, 2013).

### 3.5.1 Power transmitted by the shaft

According to Khurmi and Gupta (2005) the power transmitted by the shaft is given by Equation 3.8.

$$P = \frac{2\pi N}{60} T_s \quad (3.8)$$

It can also be written thus (Sulaiman, 2017)

$$P = \omega T_s \quad (3.9)$$

$$P = \frac{2\pi x 1400}{60} \text{ x } 22.9 = 3357.3 \text{ W}$$

Lartey (2016) explained that if power output of an electric motor is measured in watt (W), efficiency can be expressed as:

$$\eta_m = \frac{P_{out}}{P_{in}} \quad (3.10)$$

Electrical motors constructed according to National Electrical Manufacturers Association (NEMA) must meet the efficiencies in Table 3.3.

**Table 3. 3 Electric Motor efficiencies**

| Power (HP) | Minimum Nominal Efficiency (%) |
|---|---|
| 1.0 – 4.0 | 78.80 |
| 5.0 – 9.0 | 84.00 |
| 10.0 – 19.0 | 85.50 |
| 20.0 – 49.0 | 88.50 |
| 50.0 – 99.0 | 90.20 |
| 100.0 – 124.0 | 91.70 |
| > 125.0 | 92.40 |

(Source: Lartey, 2016)

The power required (4.5HP) obtained can be converted to watts is given by Equation 3.11 (Lartey, 2016).

1 horse power (HP) = 746 W (3.11)

$P_{out}$ = 4.5×746

$P_{out}$ = 3357 W

Taking efficiency as 84% from Table 3.3 and apply Equation 3.8.

$0.84 = \frac{3357}{P_{in}}$

$P_{in} = 3996.4$ W

$3996.4\text{W} = \frac{9963.4}{746} = 5.4$ HP

A 5.0 HP single-phase electric motor was selected for the machine as the horse power obtained is much closer to 5 HP. than the next motor rating which is 7.5 HP.

### 3.6 Determination of Shaft Diameter

The shafts may be designed on the basis of strength, rigidity and stiffness (Khurmi and Gupta, 2005). In designing the shaft based on strength, Khurmi and Gupta (2005) used both the twisting (torque) and bending moments.

#### 3.6.1 Determination of shaft diameter due to only twisting moment

The relation between torque and shear stress is given by Equation3.12 (Khurmi and Gupta, 2005).

$$\frac{T_s}{J} = \frac{\tau}{r} \tag{3.12}$$

The diameter of the shaft can be computed from Equation 3.13

$$T_s = \frac{\pi}{16} x\, \tau\, x\, d^3 \tag{3.13}$$

$$\tau = \frac{0.5 \times \sigma}{n} \tag{3.14}$$

$$\tau = \frac{0.5 \times 250}{3}$$

$$\tau = 42 \text{ MPa}$$

Using mild steel as the shaft material with an allowable shear stress of 42 MN/m$^2$, the shaft diameter can be obtained using Equation 3.15 (Khurmi and Gupta, 2005).

$$d = \sqrt[3]{\frac{16T_s}{\pi\tau}} \tag{3.15}$$

$$d = \sqrt[3]{\frac{16x22.9x10^3}{\pi x42}}$$

d= 14.06 mm.

### 3.6.2 Shaft diameter due to bending and twisting moment

The total weight on the shaft in Newton can be determined as;

Weight of the flywheel is 8.0×9.81= 78.5 N

Weight of the disc is 8.4×9.81= 82.4 N

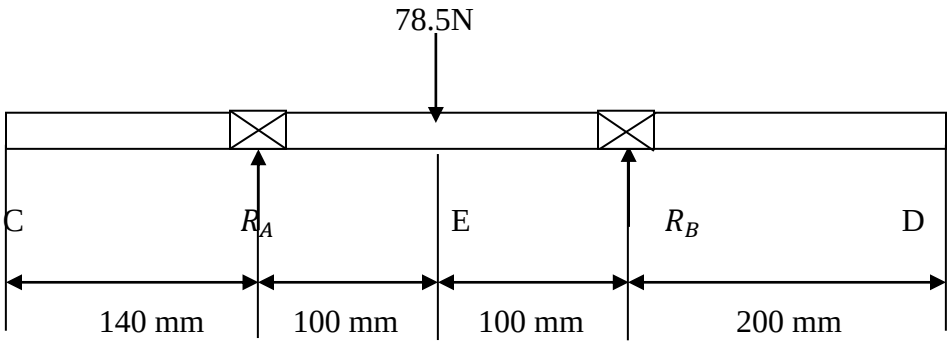


Figure 3.2 Free Body Diagram of the Rotating Shaft

Since the flywheel is at the centre between the bearings as shown in Figure 3.2, therefore, the vertical forces $R_{AV}$ and $R_{BV}$ at points A and B, are equal. Then to obtain the vertical forces $R_{AV}$ and $R_{BV}$ equate the sum of upward and downward forces.

$$R_{AV} + R_{BV} = 78.5 \text{ N} \quad (3.16)$$

We then take moment about A, $\sum M_A = 0$,

$R_{AV} + R_{BV} = 78.5$ N

$R_{AV} = R_{BV} = \frac{78.5}{2}$

$R_{AV} = R_{BV} = 39.25$ N

The shear forces are;

$V_A$= 39.25 N

$V_E$= -39.25 N

$V_B$= 0 N

Now the Bending moments at points A, B, and E;

B.M at A; $M_A = 0$ Nmm

B.M at D; $M_E = 39.25 \times 100 = 3925$ Nmm

B.M at B; $M_B = 39.25 \times (200) - 78.5 \times (200 - 100) = 0$ Nmm

To obtain equivalent twisting moment the Equation 3.17 is used (Khurmi and Gupta, 2005).

$$T_e = \sqrt{M^2 + T^2} \quad (3.17)$$

Where, M is the Maximum bending moment and T is the torque

$T_e = \sqrt{3925^2 + 22900^2}$ =23233.93 Nmm

Also $T_e = \frac{\pi}{16} \times \tau \times d^3$ taking $\tau$ as 42 MN/m$^2$

$$23233.93 = \frac{\pi}{16} \times 42 \times d^3$$

$$23233.93 = 8.247 \times d^3$$

$$d^3 = \frac{23233.93}{8.247}$$

$$d = \sqrt[3]{2817.3}$$

d = 14.12 mm

Shaft diameter due to bending and twisting moment is 14.12 mm.

### 3.6.3 Shaft diameter according to standard practice

The diameter of a shaft can be determined from the American Society of Mechanical Engineers ASME design code as used by Sulaiman (2017).

$$d^3 = \frac{16}{\pi S_s}\sqrt{(Mk_b)^2 + (Tk_t)^2} \qquad (3.18)$$

Where,$S_s$ is the shear stress, and it is taken as 42 MN/m$^2$. According to the American Society of Mechanical Engineers ASME design code: combined shock and fatigue bending ($K_b$) and torsion ($K_t$) factors for suddenly applied load, minor shock is 1.5-2 and 1-1.5 respectively. The allowable shear stress for steel with keyway is 42 MN/m$^2$ .

$$d^3 = \frac{16}{\pi x 42}\sqrt{(3925 \times 1.5)^2 + (22900 \times 1.5)^2}$$

$$= 0.12126x\sqrt{1214585156}$$

$d = \sqrt[3]{4226.02}$ = 16.16 mm. Therefore, 25 mm was selected from standard shaft sizes provided by Khurmi and Gupta (2005).

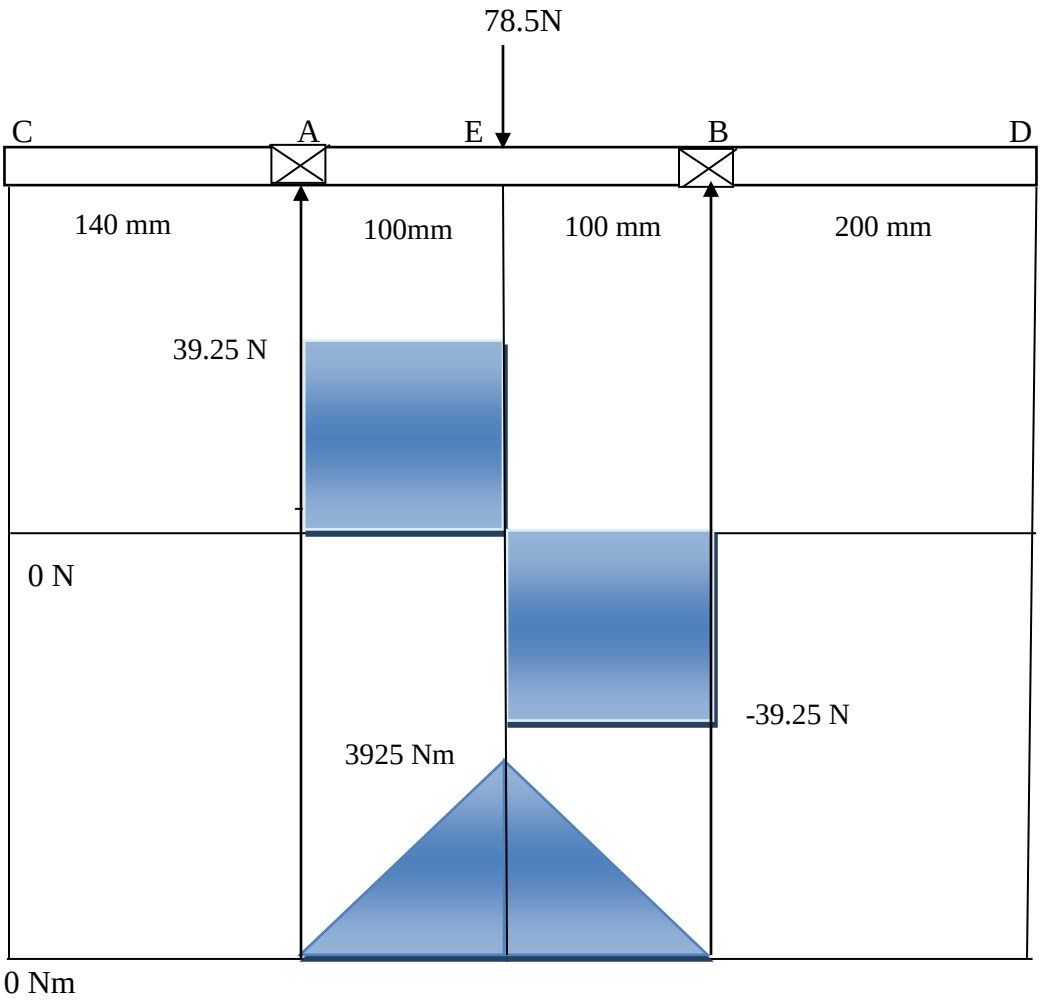


Figure 3.3 Shear forces and bending moment diagram

The shaft diameter selected for the machine is 25 mm which is more than the calculated value obtained. This implies that the shaft will have sufficient resistance to the torsion and bending stresses acting on it

### 3.7 Whirling Speed

According to Budynas and Nisbett (2015) the centrifugal force deflection of a turning shaft is caused by eccentricity which can be resisted by the shaft flexural rigidity EI. When the

deflection is minimum there will be no harm. At certain speeds, the shaft becomes unstable with deflections increasing without limit. This is the critical speed which must be avoided.

Restoring Force = Centrifugal Force (3.19)

$$ky = m(y + e)\omega^2 = my\omega^2 + me\omega^2$$

$$y = \frac{e\omega^2}{\frac{k}{m} - \omega^2}$$

But $\omega_n^2 = \frac{k}{m}$

$$y = \frac{e\omega^2}{\omega_n^2 - \omega^2} = \frac{e}{\left(\frac{\omega_n}{\omega}\right)^2 - 1}$$

When $\omega_n = \omega$ then $y = \infty$

When y tends to infinity, then the shaft will fail due to critical speed.

According to Budaynas and Nisbett (2015) the critical frequency of the shaft is given by the equation 3.20 and E = 100 GPa for the shaft material and W/m= 92.5 N/m weight of the shaft W = 78.5 N weight of point load of shaft, also the diameter of the shaft is given by 25 mm.

$$f_n = \frac{1}{2\pi}\sqrt{\frac{g}{\delta}} \quad (3.20)$$

$$I = \frac{\pi}{64}D^4$$

$I = 1.917\times 10^{-8}\text{m}^4$

According to Khurmi and Gupta (2005) the static deflection of an intrinsic shaft and shaft with point load is given by equation 3.21 and equation 3.22 respectively.

$$\delta = \frac{5}{384}\times\frac{WL^4}{EI} \tag{3.21}$$

$\delta = 1.00525\times 10^{-6}$ m

$$\delta = \frac{WL^3}{48EI} \tag{3.22}$$

$\delta = 6.8249\times 10^{-6}$ m

$$f_n = \frac{\frac{1}{2\pi}}{\sqrt{\frac{9.81}{1.00525\times 10^{-6}}}}$$

$f_n = 4907.01$ Hz

$$f_n = \frac{\frac{1}{2\pi}}{\sqrt{\frac{9.81}{6.8249\times 10^{-6}}}}$$

$f_n = 1883.24$ Hz

The Dunkerleys method as given in Equation 3.23 is used to find the critical frequency of transverse vibration (Khurmi and Gupta, 2005).

$$\frac{1}{\text{fn}^2} = \frac{1}{\text{fn1}^2} + \frac{1}{\text{fn2}^2} \tag{3.23}$$

$$\frac{1}{fn^2} = \frac{1}{4907.01^2} + \frac{1}{1883.24^2}$$

$f_n$ =1758.2 Hz

According to Khurmi and Gupta (2005) the natural frequency of vibration in revolution per second is given by Equation 3.24.

$$f_n = \frac{\omega_n}{2\pi} \quad (3.24)$$

$\omega_n = 2\pi \times f_n$

$\omega_n$ = 11047 rev/s.

$\omega = 2\pi \times 1400$

$\omega = 8796.5 \text{ rev/s}$

Therefore, since the speed of the motor in revolution per second is 8796.5 rev/s which is well below the critical speed of the shaft 11047 rev/s, then the shaft can be stable in operation (Khurmi and Gupta, 2005).

### 3.7 Design of Shaft Coupling

#### 3.7.1 Determination of hub diameter

Coupling hub diameter can be obtained using Equation 3.25 as given by Katta and Rao (2016).

$$d_1 = 1.75 \times d + 6.5 \quad (3.25)$$

$d_1 = 1.75 \times 25 + 6.5$

$d_1 = 50.25$ mm

### 3.7.2 Determination of hub length

Coupling hub length can be obtained using Equation 3.26 as given by Katta and Rao (2016).

$$L = 1.5\, d \tag{3.26}$$

$L = 1.5 \times 25$

$L = 37.5$ mm

### 3.7.3 Determination of hub thickness

Coupling hub thickness can be obtained using Equation 3.27 as stated by Katta and Rao (2016).

$$t_1 = \frac{d_1 - d}{2} \tag{3.27}$$

$$t_1 = \frac{50.25 - 25}{2}$$

$t_1 = 12.6$ mm

### 3.7.4 Determination of hub key length

To avoid the shear failure coupling hub key length can be obtained using Equation 3.28 as provided by Katta and Rao (2016).

$$T = \left(\frac{d}{4} L_K\right) \times \tau_y \times \frac{d}{2} \quad (3.28)$$

$$L_K = \frac{8 \times T}{\tau_y \times d^2}$$

$$L_K = \frac{8 \times 22.9}{42 \times 25^2}$$

$$L_K = 4.8 \text{ mm} \sim 5 \text{ mm}$$

### 3.7.5 Determination of hub key width

The hub key width can be obtained using Equation 3.29 as provided by Katta and Rao (2016).

$$W_K = \frac{d}{4} \quad (3.29)$$

$$W_K = \frac{25}{4}$$

$$W_K = 6.25 \text{ mm}$$

## 3.8 Bearing Selection

Khurmi and Gupta (2005) quoted IS: 3823–1984 for radial ball bearings and stated that the basic static radial load rating ($C_0$) is given by Equation 3.30.

$$C_0 = f_0.i.Z.D^2 \cos \alpha \quad (3.30)$$

The value of factor ($f_0$) for bearings made of hardened steel is 12.3, for radial contact and angular contact groove ball bearings (Khurmi and Gupta, 2005).

Number of rows of balls in any one bearing, is 1, *Z*, Number of ball per row is 9 for a type 207 bearing, D, Diameter of balls is 11 mm, α, $0^0$ According to the Quality Bearings and

Components (QBC) manufacturer's catalogue B620 and the value of factor ($f_0$) for bearings made of hardened steel is 12.3, for radial contact groove ball bearings (Khurmi and Gupta, 2005).

$C_0 = 12.3 \times 1 \times 9 \times 11^2 \times \cos 0^0$

$C_0 = 13.3947$ kN

According to IS: 3824 (Part 1) – 1983, the basic dynamic radial load ($C$) rating for radial ball bearings, with balls not larger than 25.4 mm in diameter, is given by

$$C = f_c (i\cos\alpha)^{0.7} Z^{2/3} D^{1.8} \quad (3.31)$$

According to the Quality Bearings and Components (QBC) catalogue B620 assessed on 15 March, 2018 (http://qbcbearings.com/TechInfo/TechInfo.htm) $f_c$ can be obtained using the relations:

$$d_m = \frac{A+B}{2} \quad (3.32)$$

$$\frac{D\cos\alpha}{d_m} \quad (3.33)$$

From Table 3.4, A and B are 72 mm and 35 mm respectively. Therefore,

$$d_m = \frac{72 + 35}{2} = 53.5 \text{ mm}$$

Then we seek the ratio $\left(\frac{D\cos\alpha}{d_m}\right)$ and locate the value of $f_c$ from Table 3.5

$$\frac{11 \times \cos 0}{53.5} = 0.2$$

**Table 3. 4 Major Features for radial ball bearings**

| Bearing No. | Dia. Mm | Exterior Dia. | Size mm |
|---|---|---|---|
| 205 | 25 | 52 | 15 |
| 305 | 25 | 62 | 17 |
| 405 | 25 | 80 | 21 |

(Khurmi and Gupta, 2005)

59.9 is selected as the value for $f_c$ from the table 3.5. The basic dynamic radial load (C) is;

$C = 59.9 \times (1\times \cos 0^{o})^{0.} \times 9^{2/3} \times 11^{1.8}$

$C = 59.9 \times 1 \times 4.33\times 74.9$

$C = 19.459$ KN

The values obtained for the static and dynamic radial loads are within the capacities of a type 205 bearing provided by Khurmi and Gupta (2005). The values are 13.7 KN and 20 KN respectively.

**Table 3.5 Values of $f_c$ for different types of bearings**

| $D \cos \alpha / d_m$ | Single row radial contact; Single & Double row angular contact, Groove Type |
|---|---|
| 0.180 | 59.9 |
| 0.20 | 59.9 |
| 0.22 | 59.6 |
| 0.24 | 59.0 |

**(Source: http://www.qbcbearings.com /TechInfo/PDF/RollingCBearings.pdf, assessed 15 March, 2018)**

According to Khurmi and Gupta (2005) the dynamic equivalent radial load for radial and angular contact bearings is given by

$$W = X.\ V.\ W_R + Y.\ W_A \quad (3.34)$$

Where, V is a rotation factor and is taken as 1 for all bearing types with rotating inner race (Khurmi and Gupta, 2005).

($W_R$) = 181.5 N (total load on bearing), and constant axial or thrust load ($W_A$) = 0, X is 1 (Khurmi and Gupta, 2005) and Y is 0.

$W = 1 \times 1 \times 181.5 = 181.5$ N

The approximate rating (or service) life of ball or roller bearings is based on Equation 3.35 as given by Khurmi and Gupta (2005);

$$L = \left(\frac{C}{W}\right)^k \times 10^6 \quad (3.35)$$

$$C = W\left(\frac{L}{10^6}\right)^{\frac{1}{k}} \quad (3.36)$$

k = 3, for ball bearings (Khurmi and Gupta, 2005).

It has been specified that this machine will operate for 8 hours per day intermittently. The bearing life in operating hours is selected as 8,000-15,000 from Table 3.6. The average life of the bearing selected is 7 years at 8 hours per day; therefore, the bearing life in hours is 13440 hours.

$L_H = 7 \times 240 \times 8 = 13440$ hours

13440 hours for 240 working days per year and life of the bearing in revolutions,

Equation 3.37 describes the relationship between the bearing life in revolutions and the bearing life in working hours as given by Khurmi and Gupta (2005).

$$L = 60\ N.\ L_H \text{ revolutions} \quad (3.37)$$

$L = 60\ N \times L_H = 60 \times 1400 \times 13440 = 1128.96x\ 10^6 rev$

**Table 3. 3 Recommended Life Value of Bearings.**

| Forms of Operation | Life in Operation |
|---|---|
| Not frequently | 500 |
| Short | 4000-8 000 |
| Alternating | 8000-15000 |
| Single shift | 15000-30000 |
| Nonstop | 30000-60000 |
| Nonstop with production capacity | 100000 |

**(Abdulkadir *et al*., 2009)**

The basic dynamic equivalent radial load service factor ($K_S$) for radial ball bearings for light shock load is 1.5 (Khurmi and Gupta, 2005). So the dynamic equivalent radial load W, becomes 181.5 x1.5 = 272.25 N

The basic dynamic load rating is given by

$C = W\left(\frac{L}{10^6}\right)^{\frac{1}{k}}$ k = 3, for ball bearings (Khurmi and Gupta, 2005).

$$FC = 272.25\left(\frac{1128.96x10^6}{10^6}\right)^{\frac{1}{3}} = 2.8348\ kN$$

The basic dynamic load is well within the range of the selected bearing type 207 which is 20 KN.

### 3.9 Frame Design

#### 3.9.1 Critical buckling load

It is known that when columns are subjected to compressive loads, they tend to fail by buckling when their critical load is attained. For a square channel angular iron column fixed at one end and free at the other end, the Euler's formula according to Khurmi and Gupta (2005) Equation 3.38 is used to determine the critical buckling load of the rig frame.

$$W_{critical} = \frac{\pi^2 E_i I_R}{4L_C 2} \tag{3.38}$$

$$I_R = \frac{bh^3}{12} \tag{3.39}$$

An angular square channel of 50 mm × 50 mm × 4 mm was used for the construction of test rig frame which was found suitable to withstand the load of the test rig components.

According to Khurmi and Gupta (2005) for a square angular channel, the moment of inertia of the angular bar is given by Equation 3.39

$$a_1 = 50 \times 4 = 200 \text{ mm}^2$$

$$a_2 = 46 \times 4 = 184 \text{ mm}^2$$

$$x_1 = \frac{4}{2} = 2 \text{ mm}$$

$$x_2 = 4 + \frac{50 - 4}{2} = 27 \text{ mm}$$

$$y_1 = \frac{50}{2} = 25 \text{ mm}$$

$$y_2 = \frac{4}{2} = 2 \text{ mm}$$

$$\bar{X} = \frac{a_1 x_1 + a_2 x_2}{a_1 + a_2} = 12.5 \text{ mm}$$

$$\bar{y} = \frac{a_1 y_1 + a_2 y_2}{a_1 + a_2} = 14 \text{ mm}$$

$$hy_1 = y_1 - \bar{y} = 11 \text{ mm}$$

$$hy_2 = \bar{y} - y_2 = 12 \text{ mm}$$

$$I_{1xx} = \frac{b_1 d_1^3}{12} + a_1 h_{y1}^2 = 65866 \text{ mm}^4$$

$$I_{2xx} = \frac{b_2 d_2^3}{12} + a_2 h_{y2}^2 = 26741.3 \text{ mm}^4$$

$$I_{XX} = I_{1xx} + I_{2xx} = 92607.3 \text{ mm}^4$$

$$hx_1 = \bar{x} - x_1 = 10.5 \text{ mm}$$

$$hx_2 = x_2 - \bar{x} = 14.5 \text{ mm}$$

$$I_{1yy} = \frac{b_1 d_1^3}{12} + a_1 h_{x1}^2 = 22316.6 \text{ mm}^4$$

$$I_{2yy} = \frac{b_2 d_2^3}{12} + a_2 h_{x2}^2 = 41930.5 \text{ mm}^4$$

$$I_{yy} = I_{1yy} + I_{2yy} = 64247{,}1 \text{ mm}^4 = 6.4247 \text{ m}^4$$

According to Khurmi and Gupta (2005) since $I_{yy}$ is less than $I_{XX}$therefore, the column will tend to buckle in y-y direction then $I_{yy}$ value is used in this design.

$w_{Cr} = mg \times \text{Factor of safety}$

$w_{Cr} = 60 \times 9.81 \times 2.5$

$w_{Cr} = 1471.5\ \text{N}$

Taking E for the material as 100GPa and 2.5 as factor of safety

$$1471.5 = \frac{\pi^2 \times 100 \times 10^3 \times 64247.1}{4 \times L_C 2}$$

$$l^2 = \frac{6.34 \times 10^{10}}{5886} = 10771231\ \text{m}$$

$l = 3282\ \text{mm} \sim 3.3\ \text{m}$

Therefore, using 3.3 m as effective length of bar, 1 m will be much more effective. The bending stress of beam of the frame will be determined by the flexural Equation 3.41(Abdulkadir *et al.,* 2009).

$$\frac{M}{I} = \frac{\sigma_b}{y} = \frac{E}{R} \qquad (3.40)$$

From the above given equation maximum bending stress can be given by Equation 3.41 (Devasane, 2018).

$$\sigma_b = \frac{My}{I} \qquad (3.41)$$

According to Khurmi and Gupta (2005) the maximum bending moment for uniformly distributed load is given by Equation 3.42

$$M_{max} = \frac{WL^2}{8} \quad (3.42)$$

$$M_{max} = \frac{1471.5 \times 0.9^2}{8}$$

$$M_{max} = 149 \text{ Nm}$$

Using Equation 3.43 maximum bending stress that can be induced due to the weight test rig components is obtained as $325 \text{ N/m}^2$ as seen below.

$$\sigma_b = \frac{149 \times 14}{6.4247}$$

$$\sigma_b = 325 \text{ N/m}^2$$

The bending strength of the mild steel beam is 250 MPa which is above the induced bending stress$325 \text{ N/m}^2$on the beam due to load of brake pad test rig components.

### 3.10 Material Selection

The selection of a material for a machine part is one of the most important decisions in design process (Budaynas and Nisbett, 2015). It is easier for the designer to base the actual material selection on previous applications (Budaynas and Nisbett, 2015). All the important material properties associated with the design, like the stiffness, strength, wear resistance and cost were all considered for the selection. Senadheera (2011) listed the basic factors to consider when selecting a material for a particular design are;

- Mechanical properties such as stiffness, strength, ductility, hardness, toughness, and fracture toughness.
- Physical properties such as density, electrical conductivity, brittleness and thermal conductivity. The physical properties of a material are traditionally defined by classical mechanics and are often called mechanical properties (Robert, 2001). The material surface properties such as strength, hardness, work hardening and ductility are very important factors for wear resistance. Wear is the term used to describe the progressive loss of materials from contacting surfaces in relative motion (Li, 2014). It must be ensured that the selected materials for contacting surfaces have sufficient wear resistance. Most of the materials selected for the machine are mild steel
- Chemical properties like corrosion resistance in various environments. Corrosion is the gradual destruction of materials (usually metals) by chemical and/or electrochemical reaction with their environment. The machine is designed to operate in a dry environment to protect components from corrosion.
- Manufacturing properties such as formability, machinability, and ease of joining.
- Cost: This is the most critical factor considered while selecting materials for this design. The machine had to satisfy all performance considerations and still be affordable to the end user. The cost as a factor is neglected when performance is the top priority, safety is also a factor that has more priority than cost. This is the case (for example) when designing nuclear plants. All the associated cost factors have been considered to get a more reasonable value. These involve processing, labour and transportation costs.

These are usually the major factors considered for selecting any material for a particular design, but some other factors may become essential depending on the particular machine designed (Senadheera, 2011).

### 3.11 Fabrication Details

#### 3.11.1 Cutting and shaping

Hacksaw was used to cut the angular iron into the various sizes required. The required height of test rig was based on the average height of human being. Scriber was used and then manually cut with the hacksaw. The shaft was cut to required length and shape using lathe operation.

#### 3.11.2 Assembling

Welding and other mechanical fastening methods were used to join the various machine components together. Welding is the process of joining two metal pieces by using heat to melt the parts together and allowing them to cool causing fusion. Welding is cheap and widely used these days in fabrication. Welding was primarily used for the frame and generally parts that are designed to be permanently joined.

The main type of mechanical fastening methods used is threaded fasteners. Threaded fasteners are bolts and nuts (Gerritsen, 2001). Threaded fasteners were used for this machine. Mechanical fastening was used to couple the bearing house to the top of the frame.

### 3.12 Machine Parts Description

#### 3.12.1 Shaft

The shaft was used to transmit power from electric motor to the brake assemble. It was machine to designed required diameter using lathe after which the shaft was cut to required length.

#### 3.12.2 Flywheel

The flywheel is positioned at centre between the two bearings. The flywheel was used to simulate weight of the vehicle so as to give it accelerated wear

#### 3.12.3 Coupling

The coupling was used to connect the shaft and electric motor outlet shaft for the purpose of transmitting the power

#### 3.12.4 Servo

The vacuum servo was used to provide assistance to operator by decreasing the braking effort. It is also called a brake booster.

#### 3.12.5 Frame

The frame is the unit of the machine on which all other components are mounted. It provides support for the machines during operation and when not in operation. Weight and strength were considered while choosing the right material for the frame. In this work, angle steel bar of 50 x 50 x 4mm (thick) is used to provide the required rigidity.

### 3.13 Testing Procedure

After the fabrication the next step is the testing and performance evaluation of the machine. Testing is necessary so that all defects present can be exposed and corrected before the performance is evaluated and the machine is commissioned for operation. After the test, the machine efficiency and wear rate of brake pads were obtained.

The equipment used for the first phase of the test procedure are: stop watch, LCD display temperature device, LCD display tachometer, semi metallic pads, ceramic pads and incorporated brake pressures gauge. The brake pads sample are coupled in to the brake assembly.

First a set of brake pads to be tested will be coupled into the calliper of the brake assembly. The shaft will then be set in motion by the electric motor. The disc and flywheel both will rotate until a stable speed of motor is achieved. When the speed stabilizes at 1400rpm, the switch will then be turned off while the motor, flywheel, disc and the shaft rotates by virtue of their inertia then the brake will be applied mechanically by depressing the brake pedal with the foot until it is brought to rest via the action of the pads against the disc. As this is done, the time taken for the shaft to come to rest will be measured and recorded. After the test, the brake pads will be brought out for visual inspection and measurements for wear in terms of reduction in thickness. The test is carried out at different speeds and different brake pressure such as 1400 rpm, 1200 rpm, 1000 rpm, 800 rpm and 600 rpm and 0.6 MPa, 0.8 MPa, 1.0 MPa, 1.2 MPa and 1.4 MPa respectively with the help of brake pressure gauge and tachometer.

### 3.14 Methods of Measuring Wear

Wear loss can be quantified using depth, area, and volume. Depth is associated with the loss of vertical height depending on force applied and varies with time. Depth was used to measure and compare wear rate because according to Michelson (2010) composite showed rapid wear which exposes the cavosurface margin and so it is used as measurement references. Digital vernier calliper was used to measure and compared the wear rate of the brake pads.

### 3.15 Cost Analysis

The total cost analysis for the fabrication of this frictional brake pad test rig is divided into material, labour and overhead cost

#### 3.15.1 Material cost

The major test rig parts that are fabricated are the frame; couplings and a detailed cost estimate of the materials used is presented in Table 3.5.

**Table 3. 4 List of materials used with price**

| No | PARTS | MATERIAL USED | SPECIFICATION (mm) | Qty | PRICE (₦) |
|---|---|---|---|---|---|
| 1 | Electric motor | | | 1 | 45000 |
| 2 | Shaft | Mild steel | 25x360 | 1 | 5,000 |
| 3 | Bearing | Cast and steel | 25 bore | 2 | 7,000 |
| 4 | Electrode | iron | Gauge 12 | 1 pack | 2,000 |
| 5 | Brake servo | | | 1 | 16000 |
| 6 | Complete brake | | | 1 | 19000 |
| 7 | Assembly Paint | | | 2 litres | 2,500 |
| 8 | Angle Frame | Mild steel | 50x5x4 | 2 | 9,000 |
| 9 | Brake pads | Ceramic and | | 16 | 24000 |
| 10 | Bolts and Nuts | Semi Metallic Mild steel | M13, M14,M15 | 18 | 2,000 |
| 11 | Brake Pressure Gauge | | M17 | 1 | 7000 |
| 12 | Digital Tachometer | | | 1 | 8000 |
| 13 | Infrared Thermometer | | | 1 | 7000 |
| 14 | Total Cost | | | | 153500 |

### 3.15.2 Total cost of construction

The work cost encounter from the construction of the testing apparatus is given below.

- Construction ₦45,200
- Painter ₦4,800
- Some expenses ₦20,000
- Total Cost = 153,500 + 45,300 + 25,000 = ₦223,500

# CHAPTER FOUR

# 4.0 RESULTS AND DISCUSSION

## 4.1 Results

### 4.1.1 Design results

The operation of this light vehicle brake pad test apparatus needs the minimum power of 3357.30 Watts. The minimum nominal efficiency of 84.0 percent from Table 3.3 of electric motor efficiencies and 5hp one phase was adopted. From ASME design code, 25.0 mm rotating shaft was adopted for this developed set up. 207 bearing having basic dynamic load capacity of 20000 N selected due to 13394 N basic dynamic load of bearing obtained.

### 4.1.2 Wear test results

The results for the brake pad wear test performed are presented in Table 4.1 and 4.2

**Table 4. 1 Effect of Speed on Brake Pad Wears at Constant Brake Pressure (0.80 MPa) After Ten Sequence of brake operations.**

| Speed (rpm) | Vertical height Reduction after 10 sequence of Brake Applications ($\times 10^{-4}$ mm) $Pad_1$ | | | | Vertical height Reduction after 10 sequence of Brake Applications ($\times 10^{-4}$ mm) $Pad_2$ | | | |
|---|---|---|---|---|---|---|---|---|
| | Samp.1 | Samp.2 | Av. | Av./10 | Samp.1 | Samp.2 | Av. | Av./10 |
| 600 | 32.0 | 34.0 | 33.0 | 3.30 | 36.0 | 40.0 | 38.0 | 3.80 |
| 800 | 35.0 | 33.0 | 34.0 | 3.40 | 39.0 | 39.80 | 39.50 | 3.99 |
| 1000 | 36.0 | 34.0 | 35.0 | 3.50 | 39.80 | 40.40 | 40.10 | 4.01 |
| 1200 | 37.0 | 39.0 | 38.0 | 3.80 | 40.0 | 41.60 | 40.80 | 4.08 |
| 1400 | 39.0 | 41.0 | 40.0 | 4.00 | 41.0 | 41.40 | 41.20 | 4.12 |

**Table 4. 2 Effect of Brake Contact Pressure on Brake Pad Wears at Constant Speed (1400 rpm) After Ten Sequence of Brake Applications.**

| Pressure (MPa) | Vertical height Reduction after 10 sequence of brake applications ($\times 10^{-4}$ mm) $Pad_1$ | | | | Vertical height Reduction after 10 sequence of brake applications ($\times 10^{-4}$ mm) $Pad_2$ | | | |
|---|---|---|---|---|---|---|---|---|
| | Samp.1 | Samp.2 | Av. | Av./10 | Samp.1 | Samp.2 | Av. | Av./10 |
| 0.6 | 38.0 | 40.0 | 39.0 | 3.9 | 39.0 | 41.0 | 40.0 | 4.0 |
| 0.8 | 39.0 | 41.20 | 40.10 | 4.01 | 41.0 | 41.60 | 41.30 | 4.13 |
| 1.0 | 40.0 | 42.40 | 41.20 | 4.12 | 41.50 | 42.50 | 42.0 | 4.20 |
| 1.2 | 42.40 | 41.20 | 41.80 | 4.18 | 43.20 | 43.80 | 43.50 | 4.35 |
| 1.4 | 42.50 | 43.50 | 43.0 | 4.3 | 44.0 | 44.0 | 44.0 | 4.40 |

### 4.1.3 Disc stopping time results

The results for average stopping time at constant brake pressure are presented in Table 4.3

**Table 4. 3 Effect of Speed on Average Stopping Time of the Disc at Constant Contact Brake Pressure (0.80 MPa) After Ten Sequence of Brake Applications.**

| Speed (rpm) | Stopping Time (Sec.) $Pad_1$ | | | $Pad_2$ | | |
|---|---|---|---|---|---|---|
| | Samp.1 | Samp. 2 | Av. | Samp. 1 | Samp. 2 | Av. |
| 600 | 1.30 | 1.06 | 1.18 | 1.20 | 1.00 | 1.10 |
| 800 | 1.35 | 1.45 | 1.40 | 1.20 | 1.30 | 1.25 |
| 1000 | 1.65 | 1.85 | 1.75 | 1.30 | 1.42 | 1.36 |
| 1200 | 1.80 | 1.98 | 1.89 | 1.70 | 1.68 | 1.69 |
| 1400 | 2.00 | 2.02 | 2.01 | 1.86 | 1.88 | 1.87 |

### 4.1.4 Disc temperature results

The results for disc temperature rise are presented in the Table 4.4

**Table 4. 4 Effects of Speed on Temperature of the Disc at Constant Contact Pressure (1.60 MPa) After Ten Sequence of Brake Applications**

| Speed (rpm) | Disc Temp. Rise After Ten Braking Sequence ($^{O}$C) Pad$_1$ | | | Disc Temp. Rise After Ten Braking Sequence ($^{O}$C) Pad$_2$ | | |
|---|---|---|---|---|---|---|
| | Sample$^1$ | Sample$^2$ | Average | Sample$^1$ | Sample$^2$ | Average |
| 600 | 56.0 | 60.0 | 58.0 | 54.0 | 58.0 | 56.0 |
| 800 | 69.0 | 65.0 | 67.0 | 67.0 | 59.0 | 63.0 |
| 1000 | 69.0 | 71.0 | 70.0 | 64.0 | 66.0 | 65.0 |
| 1200 | 75.0 | 77.0 | 76.0 | 67.0 | 69.0 | 68.0 |
| 1400 | 79.0 | 77.0 | 78.0 | 68.0 | 72.0 | 70.0 |

### 4.2 Discussion of the Results

Table 4.1 illustrate the results of wear rate in terms of vertical height reduction of the brake pad product for examination, examining the effect of disc rotational speed on vertical height reduction of brake pad specimen at brake pressure of 0.80 MPa and at the 1400 revolution per minute of 5HP single phase electric motor. The semi metallic brake pad shows 4.00 $\times 10^{-4}$ mm while ceramic brake pad shows $4.120\times10^{-4}$ mm for their brake pads vertical height reductions. It can be observed that ceramic brake pad sample have more wear when compare with semi metallic brake pad sample. At constant contact pressure of (0.80 MPa) and disc rotational speed of 1000 revolution per minute, semi metallic and ceramic brake pad vertical height reduction are $3.50\times10^{-4}$ mm and $4.010\times10^{-4}$ mm respectively for single br.ke operation. Also at disc speed of 600 revolutions per minute and constant brake effort of (0.80 MPa), wear rate are$3.3\times10^{-4}$ mm, is $3.8\times10^{-4}$ mm respectively for semi metallic and ceramic. Normally, $5.0\times10^{-4}$ mm is the vertical height reduction for one single brake application as reported by Blau (2001). From this outcome it can be

observed that the figures from this experimental setup were a little less than as described by Blau (2001).

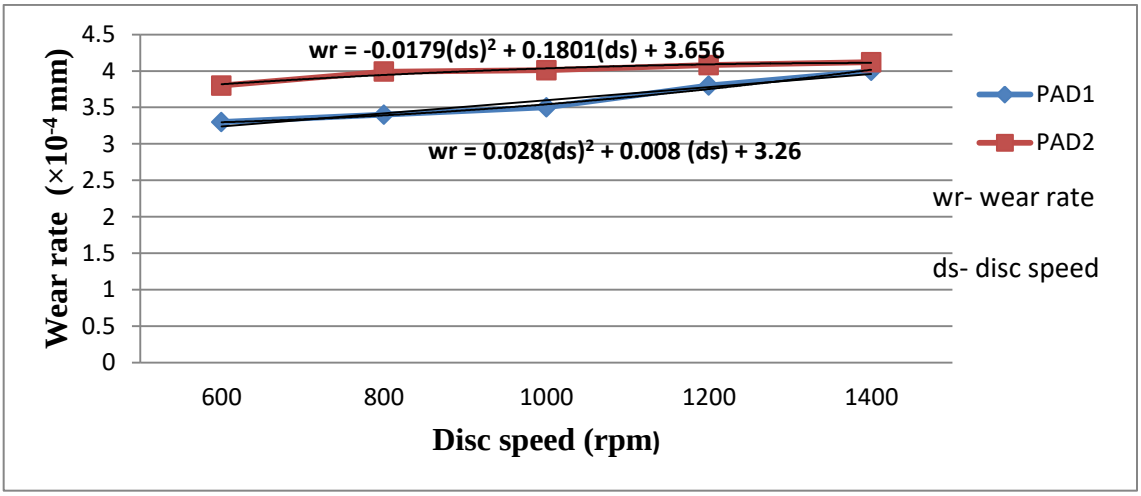


Figure 4. 1 Effect of Disc Rotational Speed on Brake Pad Wears at Invariable Pressure (0.80 MPa) After Ten sequence of Brake operation

Among the brake pad products in the market are ceramic material brake pads with ceramic as its matrix material, semi metallic and asbestos brake pads. Figure 4.1 shows ceramic pad reduce more in vertical height for every single application of brake due to its matrix material which is brittle and thereby increase its chance of wear.

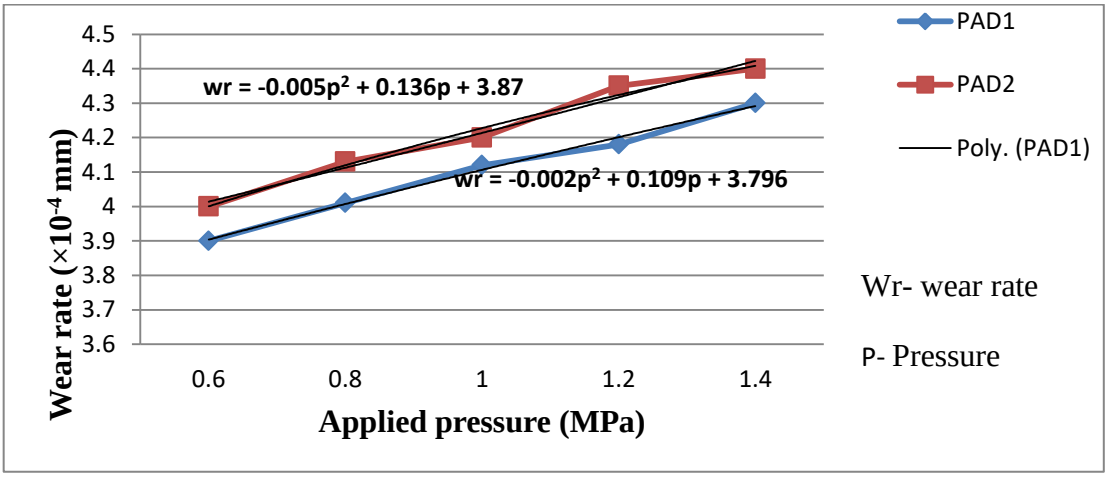


Figure 4. 2 Effect of Brake Pressure on Pads Vertical Height Reduction at Constant Speed (1400 rpm) After Ten Sequence of Brake operations.

The contour line in Figure 4.2 illustrate that the vertical height reduction reduced more as the brake applied pressure increase for every types of brake materials. The semi metallic pad wear rose from $3.90\times10^{-4}$ to $4.30\times10^{-4}$ mm for each brake operation as the applied pressure increase from 0.6 to 1.4 MPa while ceramic wear rate move from $4.0\times10^{-4}$ mm to $4.4\times10^{-4}$ mm. Aderibigbe *et al*. (2016) explained that the braking success can be established by the automobile speed reduction or time taken to standstill. Braking distance is very critical for urgent braking, it is the different between life and death. Road safety of Nigeria established that vehicle be brought to standstill three seconds distance.

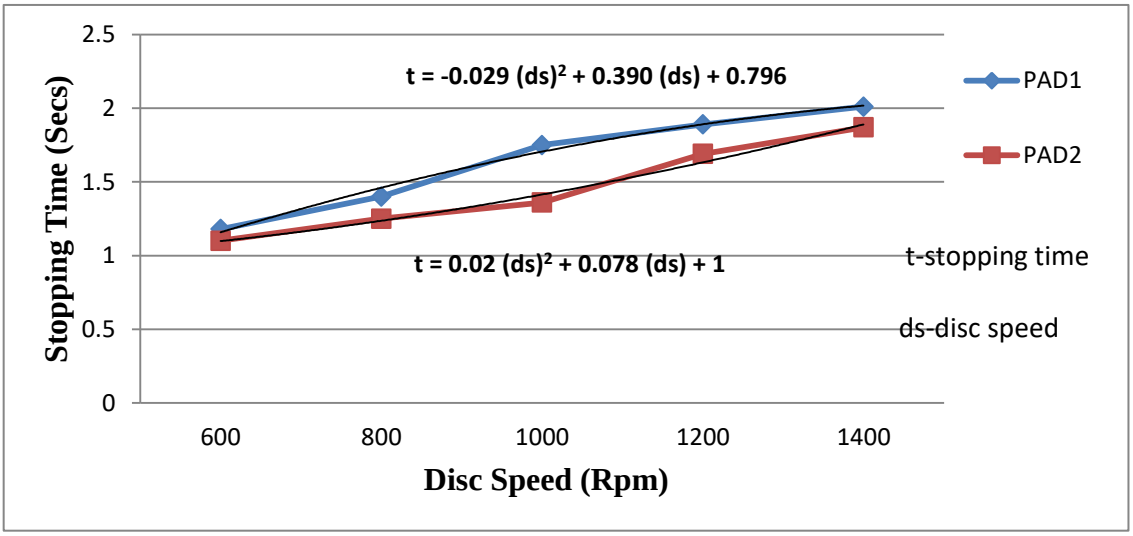


Figure 4. 3 Effect of Disc Speed on Average Stopping Time taken at Constant Contact Brake Pressure (0. 80 MPa) After Ten Sequence of Brake operation

In terms of average time taken to by rotating disc to come to standstill, the contour line in Figure 4.3 illustrate the effect of disc rotational speed on mean time taken to stop at invariable brake contact pressure (0.80 MPa) after ten sequence of operations. The profile shows the effectiveness of the ceramic brake pads over semi metallic brake pads. Uttam *et al*. (2018). Pointed out that rotating disc temperature under emergencies or continuous

braking may go tremendously high. He also asserts that as the brake heated it fades and it can be less efficient.

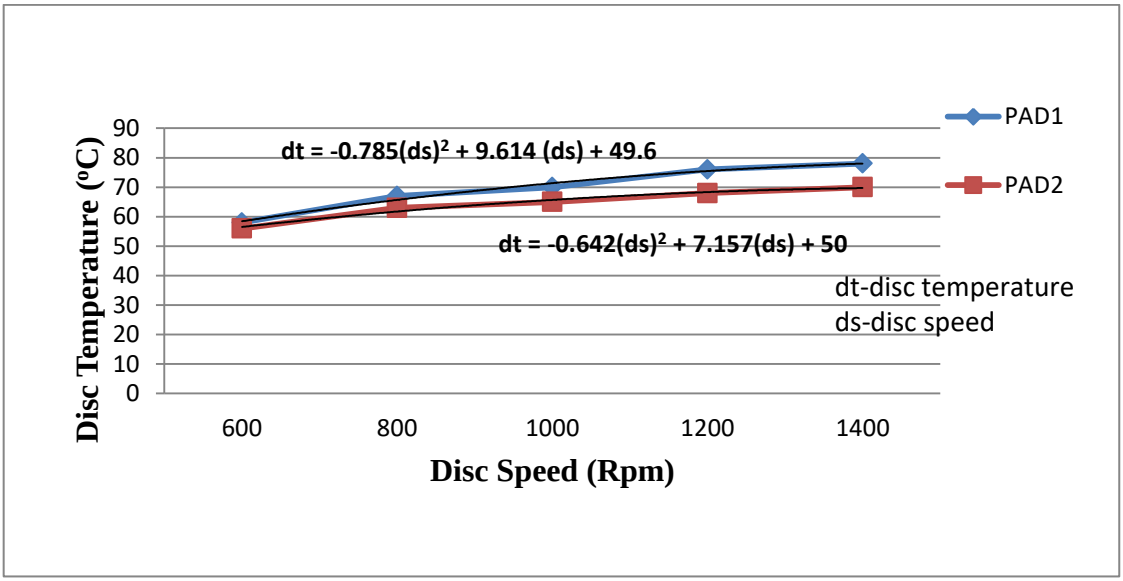


Figure 4. 4 Effects of Speed on Temperature of the Disc at Constant Contact Pressure (1.60 MPa) After Ten Sequence of Brake operation

The connection between rise in temperature of the disc and the increase in disc rotational speed is linear. Figure 4.4 demonstrate rise in temperature of semi metallic brake pads and ceramic brake pad, the graph illustrate that there is slow temperature as rotational speed increase. For closer examination, ceramic brake pads prove to be more efficient when compared with semi metallic brake pads. Ceramic brake pad has 64.40 $^{O}$C against 70.0 $^{O}$C of semi metallic brake pads.

# CHAPTER FIVE

## 5.0 CONCLUSION AND RECOMMENDATIONS

### 5.1 Conclusion

Light vehicle brake pad testing apparatus for wear rate and other frictional properties of the brake pad examination has been successfully developed. The testing of the new brake pad friction material known as aftermarket brake pads or commercially available brake pads for their accomplishment can be achieved using this testing apparatus. This experimental setup, can be used to test among other brake pad frictional properties like brake wear rate in terms of pad vertical height reduction, rotating disc temperature rise using non-contact digital tachometer, and stopping distance in terms of stopping time. The two most popular brake pads in the market were used as sample to ascertain the accomplishment of this wear testing apparatus.

The results show that:

For the two popular brake pads tested for this wear examination, the brake pad wear increase as the driver brake applied effort increase. Also wear increase as the speed of disc rotation in revolution per minute before brake application increase. (That is, wear rate is a proportional to speed and contact pressure).

For the two popular brake pads tested, temperature of the disc increase more while using semi metallic brake pads.

In time taking for rotating disc to come back to standstill, ceramic brake pads take less time in seconds as compared with semi metallic brake pads.

## 5.2 Recommendations

The following footnote were suggested for any subsequent experimentally developed brake pad test rig

1. The electric motor speed should be as high as possible so as to give the material accelerated wear for testing.
2. The measurement from the equipment such as temperature sensor, tachometer, and brake pressure gauge should display in a board for accuracy and ease of the measurements.
3. The transparent plastic casing should be designed and constructed to cover the rotating parts in order to avoid wear chips flying.

## REFERENCE


Abdulkadir, B. H., Matthew S. A., Olufemi A. O.and Ikechukwu, C. U. (2009). The design and constructionof maize threshing machine. *Assumption University Journal of Technology*, 12(3), 199 -206.

Aderibigbe, D. A., Sani, M. and Awodehinde, O. A. (2016). Design, construction and testing of an automotive brake pad test rig.*Internationjal Journal for Scientific Research and Development*.4(6), 1115–1119.

Amaren, S. G. (2013). Evaluation of the wear and thermal properties of asbestos free brake pad using periwinkles shell particles. *Usak University Journal of Material Sciences*. 2(1), 99–99.

Bhandari, V. B. (2010).*Design of machine elements.* India: Tata McGraw-Hill

Blau, P.J. (2001).*Compositions, functions and testing of friction brake materials and their additives*. Oak Ridge National Laboratory: U.S. Department of Energy (DOE). Retrieved from https://info.ornl.gov/sites/publications/Files/Pub57043.pdf

Budaynas, R. G. and Nisbett J.K. (2015).*Shigley's mechanical engineering design* (10th ed.). New York: McGraw-Hill Education.

CDX Automotive (2012). *Brakes: Fundamentals of automotive technology*. USA: Jones and Bartlett Publishers

Chatterton, S., Cangioli, F., Pennacchi, P., Vania, A., and Dang, P. V. (2016). Development of an active control system for rotating machinery by means of tilting pad journal bearings.*Proceedings of theAmerican Society of Mechanical Engineers (ASME) Turbo Expo,* (pp. 1-10). Seoul, South Korea. doi.org/10.1115/GT2016-56632

Dagwa, I.M., (2005). Design and manufacture of Automotive Disk brake pad test rig *Nigerian Journal of Engineering Research and Development*, 4(3), 15-24

Deepika, K., Reddy, C. B., and Reddy, D. R. (2013). Fabrication and performance evaluation of a composite material for wear resistance application. *International Journal of Engineering Science and Innovative Technology (IJESIT)*,2(6), 66–71.

Devasane, M. (2018, May 15). *Euler's theory of column mechanical engineering*. Retrieved from www.gradeup.co

Fecher, N., Jochen, T. and Hermann W. (2014, 14 May).*Caliper-independent investigation of brake pads.* Retrieved from https://www.azom.com/article.aspx?ArticleID=14745

Gerritsen, C. (2001). *Mechanical fastening: threaded fasteners and blind rivets*. Retrieved from http://www.ansatt.hig.no/henningj/materialteknologi/Lettvektdesign/joining%20methods/joining-mechanical-threaded%20fasteners%20and.htm.

Gudmand-Høyer, L., Bach, A., Nielsen, G. T. and Morgen, P. (1999). Tribological properties of automotive disc brakes with solid lubricants. *Wear*, 232(2), 168–175.doi.org/10.1016/S0043 -1648(99)00142-8

Gupta, S. K. (2014). *A Textbook of Automobile Engineering*. New Delhi: S. Chand & Company Pvt. Ltd.

Hoodbhoy, P. (2014). *An Introduction to Physics*. Retrieved from http://eacpe.org/content /uploads/2014/01/PHYSICS-101.pdf, September 10, 2017

Hwang, P., Wu, X. and Jeon, Y. B. (2008). Thermal–mechanical coupled simulation of a solid brake disc in repeated braking cycles. *Journal of Engineering Tribology*, 223(7), 1041-1048.doi:10.1243/13506501jet587

Ibhadode, A. O. A. and Dagwa, I. M. (2008).Development of asbestos-free friction lining material from palm kernel shell.*Journal of the Brazilian Society of Mechanical Sciences and Engineering*, 30(2), 166-173. doi.org/10.1590/S1678-58782008000200010

Idris, U. D., Aigbodion, V. S., Abubakar, I. J. and Nwoye, C. I. (2015). Eco-friendly asbestos free brake-pad using banana peels. *Journal of King Saud University - Engineering Sciences*, 27(2), 185–192. doi.org/10.1016/j.jksues.2013.06.006

Iersel, V. (2006). *Measuring brake pad friction behavior using the TR3 test bench coaches*. Eindhoven, University of Technology. Retrieved from http://www.mate.tue.nl /mate/pdfs/7138.pdf

Ivens, T. W. T. (2007). *A model for brake testing on a combustion engine powered test rig*.Eindhoven, University of Technology.Retrieved from http://www.mate.tue.nl/mate /pdfs/8833.pdf

Jamie, P. D.(2008). *How brake pads work*. Retrieved on from https://auto.howstuffworks.com /auto-parts/brakes/brake-parts/brake-pads.htm.

Katta, C. S. and Rao, K. S. (2016). Design and analysis of flange coupling. *International Journal of Professional Engineering Studies*, 1(4), 320-328.

Khurmi, R. S. and Gupta, J.K. (2005). *A text book of machine design*. New Delhi: Eurasia Publishing House (PVT.) Ltd.Khurmi, R. & Gupta, J. (2007). *Theory of machines*(8th ed.). New Delhi: Eurasia Publishing House (PVT) Ltd.

Kost, F. (2014). *Fundamentals of automotive and engine technology. Bosch Professional Automotive Information*. Wiesbaden: Springer.

Koop, C. P. (2012). *Emergency response vehicle brake testing*. Retrievedfromhttp://www.fireapparatusmagazine.com/articles/print/volume-17/issue-8/departments/apparatus-the-shops/emergency-response-vehicle-brake-testing.html

Lartey, D. (2016). *Energy efficiency in electrical drive systems: technical potentials, barriers and policy approaches for small and medium industries in Ghana.*Retrieved from https://core.ac.uk/download/pdf/39982547.pdf. 28 December, 2016

Li, C. X. (2014). *Wear and wear mechanism*. Retrieved from http://emrtk.uni-miskolc.hu/projektek/adveng/home/kurzus/korsz_anyagtech/1_konzultacio_elemei/wear_and_wear_mechanism.html.

Nwufo, O. C., Ezeji, K. M. D., Nwaiwu, C. F. &Okoronkwo, C. A. (2013). Effect of speed and contact pressure on the wear rate of automotive brake pad.*The International Journal of Engineering and Science (IJES)*, 2 (4), 72-76.

Robert, A. M. (2001). *Encyclopedia of Physical Science and Technology* (3rd ed.). USA:Academic Press

Senadheera, J. (2011). *Basic factors to consider when selecting a material for a particular design.* Retrieved from http://www.brighthubengineering.com/machine-design/55560-basic-facts-to-consider-when-selecting-a-material-for-a-particular-design/.

Sharma, P. C. and Agarwal, D. K. (2014). *Machine Design*. New Delhi, India: S. K. Kataria and Sons.

Sulaiman, I. (2017). *Development of Horizontal Shaft Hammer Mill.* Master's thesis, Federal University of Technology, Minna.

Systemtechnik brochure, (July 2017). *Brake system testing*. Retrieved from https://www.dbssystemtechnik.de/file/dbstde/11420656/bRZBksdtjreQHn6x7YHGwPE6KTA/16014440/data/product_brake_system_testing.pdf

Triches, M., Gerges, S. N. Y. and Jordan, R. (2004). Reduction of squeal noise from disc brake systems using constrained layer damping. *Journal of the Brazilian Society of Mechanical Sciences and Engineering*. 26(3), 340-348.

Van-Iersel, S. S. (2006).*Measuring brake pad friction behavior using the TR3 test bench*.Retrieved fromwww.mate.tue.nl/mate/pdfs/7138.pdf

Xiao, X., Yin, Y., Bao, J., Lu, L. and Feng, X. (2016). Review on the friction and wear of brake materials. *Advances in Mechanical Engineering*, 8(5), 1–10. doi.org/10.1177/1687814016647300